



Iron(II) and cobalt(II) complexes bearing 8-(1-aryliminoethylidene) quinaldines: Synthesis, characterization and ethylene dimerization behavior

Shengju Song^a, Tianpengfei Xiao^a, Carl Redshaw^{b,*}, Xiang Hao^a, Fosong Wang^a, Wen-Hua Sun^{a,c,**}

^aKey Laboratory of Engineering Plastics and Beijing National Laboratory for Molecular Sciences, Institute of Chemistry, Chinese Academy of Sciences, Beijing 100190, China

^bSchool of Chemistry, University of East Anglia, Norwich NR4 7TJ, UK

^cState Key Laboratory for Oxo Synthesis and Selective Oxidation, Lanzhou Institute of Chemical Physics, Chinese Academy of Sciences, Lanzhou 730000, China

ARTICLE INFO

Article history:

Received 15 February 2011

Received in revised form

20 March 2011

Accepted 29 March 2011

Keywords:

8-(1-Aryliminoethylidene)quinaldine

Iron(II) complexes

Cobalt(II) complexes

Ethylene dimerization

ABSTRACT

The series of bidentate N^N iron(II) and cobalt(II) complexes containing 8-(1-aryliminoethylidene) quinaldine derived ligands, 8-[2,6-(R¹)₂-4-R²-C₆H₂N=C (Me)]-2-Me-C₁₀H₅N, were synthesized and characterized by elemental and spectroscopic techniques. The molecular structures of **Co1** (R¹ = Me, R² = H), **Co3** (R¹ = ⁱPr, R² = H) and **Co4** (R¹ = R² = Me) were confirmed as the distorted tetrahedral by single crystal X-ray diffraction. On treatment with modified methylaluminoxane (MMAO), these complexes exhibited good catalytic activities of up to 5.71 × 10⁵ g mol⁻¹(Fe) h⁻¹ for the ethylene dimerization at 30 °C under 10 atm of ethylene, in which iron pre-catalysts produced butenes with a high selectivity for α -butene. The correlation between metal complexes, catalytic activities and the product formed were investigated under various reaction parameters.

© 2011 Elsevier B.V. All rights reserved.

1. Introduction

As major industrial reactants, α -olefins are widely used in the preparation of detergents, lubricants, plasticizers, oil-field chemicals, and monomers for co-polymerizations. The ever increasing demand of the α -olefin industry has been growing at about 5% year on year, and as a consequence, there is increasing interest in developing new catalysts and processes to produce α -olefins in both academic and industrial settings. In the past decade, significant progress has been made in the development of late transition metal catalysts for the oligomerization of ethylene. Since the discovery that 2,6-bis(arylimino)pyridine ligands (**A** in Scheme 1) can impart late transition metals, and in particular iron, with high activities for ethylene oligomerization and polymerization [1–5], a great deal of interest has focused on catalyst modification and design [6–16]. In devising late-transition metal complexes as catalysts for ethylene polymerization and oligomerization, a few models of iron and cobalt catalysts were reported [17–22]. Our group has recently reported a series of complexes with good to high

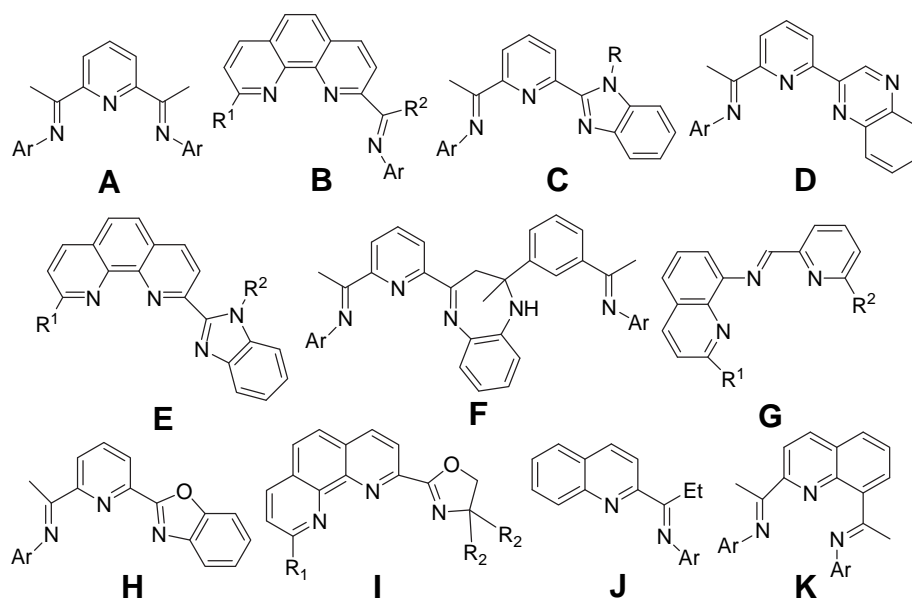
activities for ethylene polymerization and oligomerization. These systems utilize newly developed ligands (Scheme 1) such as 2-imino-1,10-phenanthrolines (**B**) [23–30], 2-(benzimidazolyl)-6-iminopyridines (**C**) [31,32], 2-quinoxaliny-6-iminopyridines (**D**) [33,34], 2-(benzimidazol-2-yl)-1,10-phenanthrolines (**E**) [35,36], 2-methyl-2,4-bis(6-iminopyridin-2-yl)-1*H*-1,5-benzodiazepines (**F**) [37,38], *N*-((pyridin-2-yl)methylene)-quinolin-8-amine (**G**) [39], 2-benzoxazolyl-6-[1-(arylimino)ethyl]pyridines (**H**) [40], 2-oxazoline- or benzoxazole-1,10-phenanthrolines (**I**) [41], 2-(1-aryliminopropylidene)quinolines (**J**) [42], 2,8-bis(imino)quinolines (**K**) [43] and 2-[1-(2,6-dibenzhydryl-4-methylphenylimino)ethyl]-6-[1-(arylimino)ethyl]pyridines [44]. Moreover, a number of the Fe(II) and Co(II) catalysts were capable of ethylene oligomerization with high activities and high selectivity of α -olefins, and can thus be considered as promising catalysts for industrial consideration. As a consequence, derivatives have been synthesized and further investigations conducted to evaluate for better performance, primarily via controlling steric and electronic influences of the ligand substituents. On the whole, those existing catalytic models of Fe(II) and Co(II) complexes have been coordinated with ligands centered via an *N*-heteroaromatic ring. We have now turned our attention to ligands containing a Schiff-base moiety at the center in combination with *N*-heteroaromatic rings.

A series of 8-(1-aryliminoethylidene) quinaldinylnickel dihalides were synthesized and found to perform with high catalytic activity for the oligomerization of ethylene [45]. Following on from this, the Fe(II) and Co(II) analogs were synthesized and characterized. The

* Corresponding author. Tel.: +44 1603 593137; fax: +44 1603 592003.

** Corresponding author. Key Laboratory of Engineering Plastics and Beijing National Laboratory for Molecular Sciences, Institute of Chemistry, Chinese Academy of Sciences, Beijing 100190, China. Tel.: +86 10 62557955; fax: +86 1062618239.

E-mail addresses: carl.redshaw@uea.ac.uk (C. Redshaw), whsun@iccas.ac.cn (W.-H. Sun).



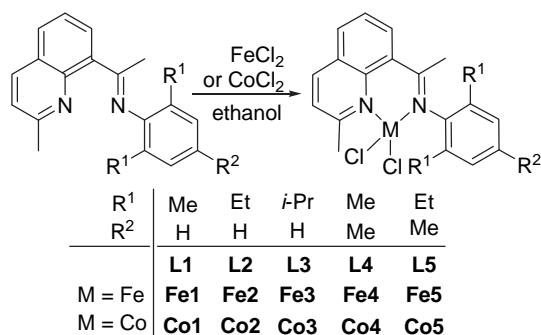
Scheme 1. Previously used ligands.

catalytic investigation showed that these Fe(II) complexes could dimerize ethylene to afford butanes in higher than 95% yields with a good selectivity for α -olefins. Herein, the synthesis and characterization of the title complexes are reported and the catalytic properties for ethylene dimerization are investigated and discussed in detail.

2. Results and discussion

2.1. Synthesis and characterization of complexes

A series of 8-(1-aryliminoethylidene)quinolines (**L1–L5**) were prepared using our previous reported procedures [45]. The iron(II) and cobalt complexes **Fe1–Fe5** and **Co1–Co5** were readily prepared by mixing the corresponding ligand and one equivalent of $\text{FeCl}_2 \cdot 4\text{H}_2\text{O}$ or CoCl_2 in ethanol at room temperature under nitrogen (Scheme 2). The resulting complexes were precipitated from the reaction solution and separated as red, yellow, or green air-stable powders. All the complexes were characterized by FT-IR spectra and elemental analysis. In the IR spectra, the stretching vibration bands of the $\text{C}=\text{N}$ of these iron(II) and cobalt(II) complexes ($1609\text{--}1625\text{ cm}^{-1}$) shifted to lower wave number and the peak intensity was greatly reduced, as compared to the corresponding ligands ($1635\text{--}1656\text{ cm}^{-1}$), indicative of coordination between the



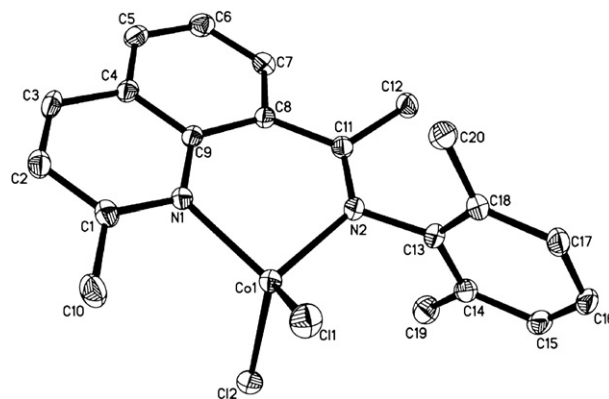
Scheme 2. Synthetic procedure.

imino nitrogen atom and the metal cation. The unambiguous structures were confirmed by single-crystal X-ray diffraction analysis.

2.2. Crystal structures

Single crystals of complexes **Co1**, **Co3** and **Co4** suitable for X-ray diffraction analysis were obtained by slow diffusion of diethyl ether into methanol solutions. The crystal structures are shown in Figs. 1–3, and selected bond lengths and angles are collected in Table 1.

In the structure of **Co1**, the geometry around the cobalt center can be described as distorted tetrahedral, in which the cobalt atom is coordinated by one bidentate N,N ligand and two chlorine atoms. The quinoline plane with the aryl ring makes a dihedral angle of 79.01° and the cobalt center slightly deviates by 0.143Å from the quinoline plane. Meanwhile, the quinoline plane with the aryl ring makes dihedral angles of 59.31° and 81.88° in **Co3** and **Co4**, respectively. The slight differences of bond distances and angles around the cobalt center were caused by the presence of different substituents on the ligands, which also affected the catalytic behavior of the cobalt complexes.

Fig. 1. Molecular structure of **Co1**. Thermal ellipsoids are shown at the 30% probability level. Hydrogen atoms have been omitted for clarity.

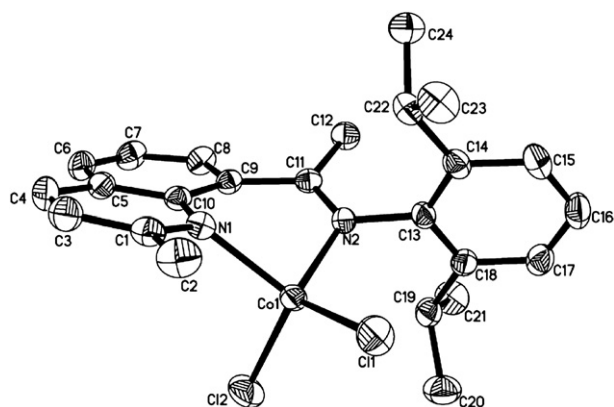


Fig. 2. Molecular structure of **Co3**. Thermal ellipsoids are shown at the 30% probability level. Hydrogen atoms have been omitted for clarity.

2.3. Reactions with ethylene

2.3.1. Ethylene dimerization by iron complexes

The influence of various alkylaluminum reagents such as methylaluminoxane (MAO), modified methylaluminoxane (MMAO) and diethylaluminum chloride (Et_2AlCl) as co-catalysts was evaluated for ethylene activation by **Fe3**. The results are summarized in Table 2. The catalytic system **Fe3**/MMAO exhibited highest activities, whilst the systems **Fe3**/ Et_2AlCl or MAO showed no activity. Herein, MMAO as co-catalyst was further explored.

The influence of reaction parameters such as the Al/Fe molar ratio and the reaction temperature on the ethylene dimerization activity was investigated (Table 2). For the iron complex **Fe3**, the enhancement of the Al/Fe molar ratio from 1000 to 1500 resulted in an increase in the catalytic activity (entries 3–5, Table 2), which may be attributed to the fact that the MMAO scavenged any adventitious water and impurities present in the solvent at low Al/Fe ratios, and the iron complex required more co-catalyst to be activated. Further increasing the molar ratio to 3500 resulted in decreased activities with the optimum condition using an Al/Fe ratio of 1500. This observation could be traced to the increasing amount of isobutyl groups present, which come from the MMAO, resulting in the generated species hindering the insertion reaction of ethylene due to increased steric bulk [31,46,47]. Meanwhile, it is noteworthy that the α -C₄ selectivity of **Fe3** decreased slightly with increasing Al/Fe molar ratio. Notably, for the complex **Fe3**, the varied amounts of co-catalyst showed no clear impact on the proportion of the C₄ component in the products. An Al/Fe ratio of 1500 appeared as a good trade-off between the activity and selectivity. Elevating the reaction temperature from 30 °C to 60 °C resulted in a large decrease

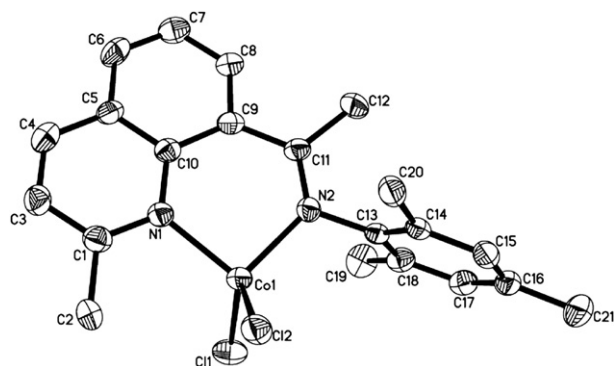


Fig. 3. Molecular structure of **Co4**. Thermal ellipsoids are shown at the 30% probability level. Hydrogen atoms have been omitted for clarity.

Table 1
Selected bond lengths(Å) and angles(°) for **Co1**, **Co3** and **Co4**.

	Co1	Co3	Co4
Bond lengths (Å)			
Co(1)–N(1)	2.025(3)	2.0398(19)	2.021(3)
Co(1)–N(2)	1.997(3)	2.0012(19)	1.996(3)
Co(1)–Cl(1)	2.2421(14)	2.2056(8)	2.2381(14)
Co(1)–Cl(2)	2.2443(13)	2.2309(9)	2.2596(12)
N(1)–C(1)	1.350(5)	1.338(3)	1.342(5)
N(1)–C(10)	1.376(5)	1.380(3)	1.388(5)
N(2)–C(11)	1.290(5)	1.287(3)	1.302(5)
N(2)–C(13)	1.456(5)	1.451(3)	1.452(5)
Bond angles(°)			
N(2)–Co(1)–N(1)	94.25(14)	90.76(7)	95.75(14)
N(2)–Co(1)–Cl(1)	107.59(11)	109.31(6)	114.91(11)
N(1)–Co(1)–Cl(1)	115.62(11)	122.64(6)	110.24(11)
N(2)–Co(1)–Cl(2)	113.57(11)	114.15(6)	109.64(10)
N(1)–Co(1)–Cl(2)	111.38(10)	103.37(6)	113.06(10)
Cl(1)–Co(1)–Cl(2)	113.03(5)	114.56(3)	112.26(5)
C(1)–N(1)–C(10)	120.0(3)	120.2(2)	119.5(3)
C(1)–N(1)–Co(1)	117.5(3)	120.89(16)	117.2(3)
C(10)–N(1)–Co(1)	122.3(3)	113.44(14)	123.1(3)
C(11)–N(2)–C(13)	121.1(4)	121.19(18)	119.6(3)
C(11)–N(2)–Co(1)	126.9(3)	122.84(15)	125.8(3)
C(13)–N(2)–Co(1)	112.0(3)	115.97(14)	114.6(2)

in productivity (entries 5 and 10–12 in Table 2), suggesting that the active centers are thermally unstable [48].

The nature of the ligands present has a large influence on the catalyst performance. To compare the influence of the ligand environment on the catalytic behavior of the iron pre-catalysts, all iron pre-catalysts **Fe1**–**Fe5** were investigated under optimum reaction condition of molar ratio MMAO/Fe at 1500:1, 30 °C and 10 atm ethylene (Table 2). The catalytic activities of the iron complexes were significantly affected by the ligand environments, and an activity order of **Fe3** > **Fe5** > **Fe4** > **Fe2** > **Fe1** was observed. The steric effects of ligands played a major role, especially substituents at the *ortho*-position of the *N*-bound aryl group. The bulkier the substituents, the higher the activity observed, which was in line with observations for the iron pre-catalysts ligated by 2-(1-methyl-2-benzimidazolyl)-6-(1-(arylimino)ethyl)pyridines [31] and 2-(1*H*-2-benzimidazolyl)-6-(1-(arylimino)ethyl) pyridines [49]. For pre-catalysts with less bulky substituents, the iron center was more exposed not only to ethylene but also to other impurities,

Table 2
Ethylene dimerization with pre-catalysts **Fe1**–**Fe5**^a

Entry	T/°C	Co-cat.	Cat.	Al/Fe	Activity ^b	Oligomer distribution ^c (%)		
						α -C ₄	C ₄ / Σ C	C ₆ / Σ C
1	30	MAO	Fe3	1000	–	–	–	–
2	30	Et_2AlCl	Fe3	200	–	–	–	–
3	30	MMAO	Fe3	1000	1.18	93.6	99.2	0.8
4	30	MMAO	Fe3	1200	3.01	99.0	99.1	0.9
5	30	MMAO	Fe3	1500	5.71	99.6	97.5	2.5
6	30	MMAO	Fe3	2000	5.51	98.5	97.2	2.8
7	30	MMAO	Fe3	2500	4.01	98.8	99.6	0.4
8	30	MMAO	Fe3	3000	3.83	100	100	–
9	30	MMAO	Fe3	3500	3.09	97.2	99.6	0.4
10	40	MMAO	Fe3	1500	4.64	95.5	96.6	3.2
11	50	MMAO	Fe3	1500	3.52	96.4	95.7	4.3
12	60	MMAO	Fe3	1500	0.78	94.6	96.8	3.2
13	30	MMAO	Fe1	1500	4.37	99.1	97.7	2.3
14	30	MMAO	Fe2	1500	4.77	98.9	97.8	2.2
15	30	MMAO	Fe3	1500	5.71	99.6	97.5	2.5
16	30	MMAO	Fe4	1500	4.94	98.2	99.1	0.9
17	30	MMAO	Fe5	1500	4.97	99.3	98.5	1.5

^a Conditions: 5 μmol Fe, 10 atm ethylene, 30 min, 100 mL toluene.

^b $10^5 \text{ g} \cdot \text{mol}^{-1}(\text{Fe}) \cdot \text{h}^{-1}$.

^c Determined by GC; Σ C denotes the total amounts of oligomers.

Table 3
Ethylene dimerization with pre-catalysts **Co1–Co5**^a

Entry	T/°C	Co-catalyst	Cat.	Al/Co	Activity ^b	Oligomer distribution ^c (%)		
						α -C ₄	C ₄ / Σ C	C ₆ / Σ C
1	20	MAO	Co3	1000	0.24	92.0	76.8	23.2
2	20	Et ₂ AlCl	Co3	200	0.36	50.3	98.2	1.8
3	20	MMAO	Co3	1000	2.01	43.2	92.0	8.0
4	20	MMAO	Co3	1500	2.40	45.2	98.5	1.5
5	20	MMAO	Co3	2000	3.21	63.0	98.9	1.1
6	20	MMAO	Co3	2250	4.26	51.2	98.8	1.2
7	20	MMAO	Co3	2500	4.89	59.9	98.4	1.6
8	20	MMAO	Co3	2750	3.66	50.3	98.6	1.4
9	20	MMAO	Co3	3000	3.19	50.3	98.7	2.3
10	20	MMAO	Co3	3500	2.15	53.0	94.6	1.6
11	30	MMAO	Co3	2500	3.88	53.3	98.9	1.1
12	40	MMAO	Co3	2500	2.20	68.6	98.7	1.3
13	50	MMAO	Co3	2500	1.97	80.4	98.3	1.7
14	20	MMAO	Co1	2500	3.03	58.4	98.2	1.8
15	20	MMAO	Co2	2500	3.34	57.2	96.5	3.5
16	20	MMAO	Co3	2500	4.89	59.9	98.4	1.6
17	20	MMAO	Co4	2500	3.07	57.6	98.2	1.8
18	20	MMAO	Co5	2500	3.56	56.5	97.2	2.8

^a Conditions: 5 μ mol Co, 10 atm ethylene, 30 min, 100 mL toluene.^b 10⁵ g·mol⁻¹(Co)·h⁻¹.^c Determined by GC; Σ C denotes the total amounts of oligomers.

which resulted in the deactivation of the active species. In addition, bulkier substituents might be helpful due to their enhanced solubility properties. Introducing one methyl group at the *para*-position of the aryl group led to a slightly higher activity (entries 16 and 17

Table 4
Crystal data and structure refinement for pre-catalysts **Co1**, **Co3** and **Co4**.

	Co1	Co3	Co4
Cryst color	Green	Green	Green
Empirical formula	C ₂₀ H ₂₀ Cl ₂ CoN ₂	C ₂₄ H ₂₈ Cl ₂ CoN ₂	C ₂₁ H ₂₂ Cl ₂ CoN ₂
fw	418.21	474.31	432.24
T (K)	173(2)	293(2)	293(2)
Wavelength (Å)	0.71073	0.71073	0.71073
Cryst syst	Orthorhombic	Monoclinic	Monoclinic
Space group	Pbca	C2/c	P2(1)/c
a (Å)	14.711(3)	29.757(6)	12.007(2)
b (Å)	15.083(3)	10.487(2)	12.966(3)
c (Å)	17.342(4)	15.019(3)	16.588(3)
α (°)	90	90	90
β (°)	90	104.17(3)	103.00(3)
γ (°)	90	90	90
V (Å ³)	3848.0(13)	4544.3(16)	2516.3(9)
Z	8	8	4
Dcalcd. (mgm ⁻³)	1.444	1.387	1.141
μ (mm ⁻¹)	1.174	1.003	0.900
F(000)	1720	1976	892
Cryst size (mm)	0.40 × 0.30 × 0.20	0.25 × 0.20 × 0.08	0.20 × 0.20 × 0.09
θ range (°)	2.35–30.02	1.41–27.48	1.74–27.45
Limiting indices	–14 ≤ h ≤ 20 –14 ≤ k ≤ 21 –24 ≤ l ≤ 24	–26 ≤ h ≤ 38 –13 ≤ k ≤ 13 –19 ≤ l ≤ 19	–12 ≤ h ≤ 15 –16 ≤ k ≤ 16 –21 ≤ l ≤ 16
No. of rflns collected	38256	18031	20193
No. unique rflns	5615 (0.0800)	5217(0.0320)	5634(0.0746)
[R(int)]			
Completeness to θ (%)	99.9%	99.8%	97.9%
Abs corr	None	None	None
Data/restraints /params	5615/0/226	5217/0/262	5634/0/235
Goodness of fit on F ²	1.313	1.168	0.993
Final R indices	R1 = 0.0970 wR2 = 0.1868	R1 = 0.0456 wR2 = 0.1235	R1 = 0.0678 wR2 = 0.1702
R indices (all data)	R1 = 0.1065 wR2 = 0.1910	R1 = 0.0475 wR2 = 0.1249	R1 = 0.0878 wR2 = 0.1838
Largest diff peak and hole (e Å ⁻³)	0.564 and –0.543	0.409 and –0.596	0.637 and –0.562

in Table 2), with the activity order as **Fe4** > **Fe1** and **Fe5** > **Fe2**. Such phenomena were also observed for iron pre-catalysts ligated by 2-quinoxaliny-6-iminopyridines [33] and 2-(1-isopropyl-2-benzimidazolyl)-6-(1-(arylimino)ethyl)pyridines [50].

2.3.2. Ethylene dimerization by cobalt complexes

In a similar procedure, complex **Co3** was used to explore suitable co-catalysts (entries 1–3 in Table 3) for optimum dimerization conditions. The **Co3**/MAO catalytic system displayed low catalytic activities for ethylene dimerization with high selectivity for butanes at 10 atm of ethylene pressure. In the presence of MMAO, the higher activity was obtained, but with lower selectivity for α -olefins.

The catalytic system **Co3**/MMAO was typically investigated with varying reaction conditions. When the Al/Co molar ratio of **Co3** was enhanced from 1000 to 3500 (entries 3–10 in Table 3), the optimum activity was observed at 2500, meanwhile the selectivity for α -butene was relatively lower. As the ethylene dimerization is a highly exothermic reaction, the reaction temperature significantly affects the catalytic activity. With increasing reaction temperature, the catalytic activity gradually decreased, which may be attributed to the decomposition of the active sites and lower ethylene solubility at higher temperature (entries 7, 11–13 in Table 3). However, the selectivity for α -olefins showed an enhancement, whilst the proportion of C₄ was only slightly affected. Complex **Co3** exhibited an activity of 4.89 × 10⁵ g mol⁻¹(Co) h⁻¹ at the Al/Co molar ratio of 2500:1 and 20 °C under 10 atm of ethylene pressure.

In a similar manner to the iron complexes, ethylene dimerization by **Co1–Co5**/MMAO systems was investigated under optimum condition (Al/Co molar ratio of 2500:1 at 20 °C). In general, for these cobalt systems, relatively lower activities were exhibited with lower selectivity for α -butene compared to their iron analogs (entries 14–18 in Table 3). The order the activities observed for the cobalt pre-catalysts was consistent with the iron analogs above.

3. Conclusion

The series of cobalt(II) and iron(II) complexes bearing 8-(1-aryliminoethylidene)quinaldines were synthesized and fully characterized by FT-IR, elemental analyses and single crystal X-ray diffraction. Upon activation with MMAO, all the iron(II) and cobalt(II) complexes showed good activity in ethylene dimerization, in which the iron(II) pre-catalysts showed higher activities and better selectivity for α -butene than did their cobalt(II) analogs. Bulky substituents resulted in better catalytic activities, with additional substituents at the *para*-position of the aryl group yielding higher activity.

4. Experimental section

4.1. General considerations

All manipulations of air- and moisture-sensitive compounds were performed under a nitrogen atmosphere using standard Schlenk techniques. The 8-(1-aryliminoethylidene)quinaldines (**L1–L5**) were prepared according to our reported procedure [45]. Toluene was refluxed over sodium-benzophenone and distilled under argon prior to use. Methylaluminoxane (MAO, 1.46 M solution in toluene) and modified methylaluminoxane (MMAO, 1.93 M in heptane, 3A) were purchased from Akzo Nobel Corp. Diethylaluminum chloride (Et₂AlCl, 1.7M in toluene) was purchased from Acros Chemicals. FT-IR spectra were recorded on a Perkin–Elmer System 2000 FT-IR spectrometer. Elemental analyses were carried out using a Flash EA 1112 microanalyzer. GC analyses were performed with a Varian CP-3800 gas chromatograph equipped with a flame ionization detector and a 30 m (0.2 mm

i.d., 0.25 μm film thickness) CP-Sil 5 CB column. The yields of oligomers were calculated by referencing with the mass of the solvent, on the basis of the prerequisite that the mass of each fraction was approximately proportional to its integrated areas in the GC trace. Selectivity for the linear α -olefin was defined as (amount of linear α -olefin of all fractions)/(total amount of oligomer products) in percent.

4.2. Synthesis of complexes

4.2.1. [2,6-dimethyl-N-(1-(2-methylquinoline-8-yl)ethylidene)benzenamine]FeCl₂ (**Fe1**)

To a solution of the ligand (E)-2,6-dimethyl-N-(1-(2-methylquinoline-8-yl)ethylidene)benzenamine (0.288, 1.0 mmol) in ethanol (5 mL), FeCl₂·4H₂O (0.199 g, 1.0 mmol) was added under nitrogen. The reaction mixture was stirred at room temperature for 12 h to afford a precipitate from the reaction mixture. The resulting precipitate was filtered off, washed twice with diethyl ether and dried in vacuum to furnish the pure product. **Fe1** was obtained as a red solid in 75% yield. (Found: C, 57.75; H, 4.97; N, 6.51. C₂₀H₂₀Cl₂N₂Fe (414.04) requires C, 57.86; H, 4.86; N, 6.75%); FT-IR (Diamond disc, cm⁻¹) 1618, 1596, 1565, 1505, 1467, 1371, 1280, 1203, 1185, 843, 794, 772.

4.2.2. [2,6-diethyl-N-(1-(2-methylquinoline-8-yl)ethylidene)benzenamine]FeCl₂ (**Fe2**)

Fe2 was obtained as a yellow powder in 73% yield. (Found: C, 59.42; H, 5.56; N, 6.21. C₂₂H₂₄Cl₂FeN₂ (442.07) requires C, 59.62; H, 5.46; N, 6.32%); FT-IR (Diamond disc, cm⁻¹): 2965, 1625, 1600, 1507, 1453, 1368, 1288, 1220, 848, 760.

4.2.3. [2,6-diisopropyl-N-(1-(2-methylquinoline-8-yl)ethylidene)benzenamine]FeCl₂ (**Fe3**)

Fe3 was obtained as a yellow powder in 86% yield. (Found: C, 60.99; H, 6.10; N, 5.93. C₂₄H₂₈Cl₂FeN₂ (470.10) requires C, 61.17; H, 5.99; N, 5.94%); FT-IR (Diamond disc, cm⁻¹): 2963, 1620, 1598, 1514, 1455, 1365, 1290, 1178, 850, 765.

4.2.4. [2,4,6-trimethyl-N-(1-(2-methylquinoline-8-yl)ethylidene)benzenamine]FeCl₂ (**Fe4**)

Fe4 was obtained as a red powder in 78% yield. (Found: C, 58.53; H, 5.27; N, 6.32. C₂₁H₂₂Cl₂FeN₂ (428.05) requires C, 58.77; H, 5.17; N, 6.53%); FT-IR (Diamond disc, cm⁻¹) 2915, 1617, 1591, 1564, 1508, 1371, 1274, 1204, 1148, 850, 767.

4.2.5. [2,6-diethyl-4-methyl-N-(1-(2-methylquinoline-8-yl)ethylidene)benzenamine]FeCl₂ (**Fe5**)

Fe5 was obtained as a yellow powder in 86% yield. (Found: C, 60.34; H, 5.79; N, 6.07. C₂₃H₂₆Cl₂FeN₂ (456.08) requires C, 60.42; H, 5.73; N, 6.13%); FT-IR (Diamond disc, cm⁻¹) 1614, 1497, 1419, 1374, 1249, 1110, 1059, 864, 682.

4.2.6. [2,6-dimethyl-N-(1-(2-methylquinoline-8-yl)ethylidene)benzenamine]CoCl₂ (**Co1**)

To a solution of the ligand (E)-2,6-dimethyl-N-(1-(2-methylquinoline-8-yl)ethylidene)benzenamine (0.288 g, 1.0 mmol) in ethanol (5 mL), CoCl₂ (0.130 g, 1 mmol) was added. The reaction mixture was stirred at room temperature for 12 h to afford a green precipitate from the reaction mixture. The resultant precipitate was collected, washed with diethyl ether and dried in vacuum. **Co1** was obtained as a green powder in 80% yield. (Found: C, 58.22; H, 5.24; N, 6.34. C₂₀H₂₀Cl₂CoN₂ (431.05) requires C, 58.35; H, 5.13; N, 6.48%); FT-IR (Diamond disc, cm⁻¹) 1615, 1586, 1560, 1513, 1455, 1272, 1207, 848, 770.

4.2.7. [2,6-diethyl-N-(1-(2-methylquinoline-8-yl)ethylidene)benzenamine]CoCl₂ (**Co2**)

Co2 was obtained as a green powder in 79% yield. (Found: C, 59.14; H, 5.45; N, 6.21. C₂₂H₂₄Cl₂CoN₂ (445.06) requires C, 59.21; H, 5.42; N, 6.28%); FT-IR (Diamond disc, cm⁻¹) 1609, 1584, 1556, 1510, 1443, 1328, 1271, 1203, 858, 771.

4.2.8. [2,6-diisopropyl-N-(1-(2-methylquinoline-8-yl)ethylidene)benzenamine]CoCl₂ (**Co3**)

Co3 was obtained as a green powder in 85% yield. (Found: C, 60.89; H, 5.94; N, 5.89. C₂₄H₂₈Cl₂CoN₂ (473.10) requires C, 60.77; H, 5.95; N, 5.91%); FT-IR (Diamond disc, cm⁻¹) 1617, 1591, 1563, 1452, 1366, 1325, 1272, 1248, 1202, 849, 804, 762.

4.2.9. [2,4,6-trimethyl-N-(1-(2-methylquinoline-8-yl)ethylidene)benzenamine]CoCl₂ (**Co4**)

Co4 was obtained as a green powder in 77% yield. (Found: C, 58.35; H, 5.17; N, 6.42. C₂₁H₂₂Cl₂CoN₂ (431.05) requires C, 58.35; H, 5.13; N, 6.48%); FT-IR (Diamond disc, cm⁻¹) 1617, 1582, 1561, 1514, 1376, 1273, 1205, 853, 774.

4.2.10. [2,6-diethyl-4-methyl-N-(1-(2-methylquinoline-8-yl)ethylidene)benzenamine]CoCl₂ (**Co5**)

Co5 was obtained as a green powder in 84% yield. (Found: C, 60.00; H, 5.71; N, 6.05. C₂₃H₂₆Cl₂CoN₂ (459.08) requires C, 60.01; H, 5.69; N, 6.09%); FT-IR (Diamond disc, cm⁻¹) 1614, 1587, 1561, 1510, 1456, 1267, 1208, 849, 774.

4.3. General procedure for ethylene dimerization

Ethylene dimerization at 10 atm ethylene pressure was performed in a stainless steel autoclave (0.25 L capacity) equipped with a mechanical stirrer, a temperature controller and gas ballast through a solenoid valve for continuous feeding of ethylene at constant pressure. The catalyst precursor was dissolved in 50 mL toluene in a Schlenk tube stirred with a magnetic stirrer and injected into the reactor under an ethylene flux. With adding the aluminium co-catalyst and more toluene in order to maintain a total volume of 100 mL toluene, the reaction temperature had been adapted to the required value, then ethylene with the desired pressure was introduced to initiate the reaction. After the reaction mixture had been stirred for the desired period of time, the reaction was stopped and about 1 mL of the reaction solution was collected, terminated by the addition of 10% aqueous hydrogen chloride. The organic layer was analyzed by gas chromatography (GC) for determining the composition and mass distribution of the oligomers obtained.

4.4. Crystal structure determinations

Single-crystals of **Co1**, **Co3** and **Co4** suitable for X-ray diffraction studies were obtained by the slow diffusion of diethyl ether into their methanol solutions. Single-crystal X-ray diffraction studies were carried out on a Rigaku RAXIS Rapid IP diffractometer using graphite monochromated Mo-K α radiation ($\lambda = 0.71073 \text{ \AA}$). Cell parameters were obtained by global refinement of the positions of all collected reflections. Intensities were corrected for Lorentz and polarization effects and empirical absorption. The structures were solved by direct methods and refined by full-matrix least squares on F^2 . All non-hydrogen atoms were refined anisotropically. All hydrogen atoms were placed in calculated positions. Structure solution and refinement were performed by using the SHELXL-97 package [51]. Crystal data and processing parameters for the complexes **Co1**, **Co3** and **Co4** are summarized in Table 4.

Acknowledgments

This work is supported by MOST 863 program No. 2009AA033601. The EPSRC are thanked for the awarded of a travel grant (to CR).

Appendix A. Supplementary material

CCDC 812782, 812783, and 812784 contain the supplementary crystallographic data for the complexes **Co1**, **Co3** and **Co4**. These data can be obtained free of charge from The Cambridge Crystallographic Data Centre via www.ccdc.cam.ac.uk/data_request/cif.

References

- [1] B.L. Small, M. Brookhart, A.M.A. Bennet, *J. Am. Chem. Soc.* 120 (1998) 4049–4050.
- [2] B.L. Small, M. Brookhart, *Macromolecules* 32 (1999) 2120–2130.
- [3] B.L. Small, M. Brookhart, *J. Am. Chem. Soc.* 120 (1998) 7143–7144.
- [4] G.J.P. Britovsek, V.C. Gibson, B.S. Kimberley, P.J. Maddox, S.J. McTavish, G.A. Solan, A.J.P. White, D.J. Williams, *Chem. Commun.* (1998) 849–850.
- [5] G.J.P. Britovsek, M. Bruce, V.C. Gibson, B.S. Kimberley, P.J. Maddox, S. Mastroianni, S.J. McTavish, C. Redshaw, G.A. Solan, S. Strömberg, A.J.P. White, D.J. Williams, *J. Am. Chem. Soc.* 121 (1999) 8728–8740.
- [6] V.C. Gibson, S.K. Spitzmesser, *Chem. Rev.* 103 (2003) 283–315.
- [7] G.J.P. Britovsek, V.C. Gibson, D.F. Wass, *Angew. Chem. Int. Ed.* 38 (1999) 428–447.
- [8] S.D. Ittel, L.K. Johnson, M. Brookhart, *Chem. Rev.* 100 (2000) 1169–1203.
- [9] S. Mecking, *Angew. Chem. Int. Ed.* 40 (2001) 534–540.
- [10] S. Park, Y. Han, S.K. Kim, J. Lee, H.K. Kim, Y. Do, *J. Organomet. Chem.* 689 (2004) 4263–4276.
- [11] C. Bianchini, G. Giambastiani, G.I. Rios, G. Mantovani, A. Meli, A.M. Segarra, *Coord. Chem. Rev.* 250 (2006) 1391–1418.
- [12] V.C. Gibson, C. Redshaw, G.A. Solan, *Chem. Rev.* 107 (2007) 1745–1776.
- [13] F. Speiser, P. Braustein, L. Saussine, *Acc. Chem. Res.* 38 (2005) 784–793.
- [14] S. Jie, W.-H. Sun, T. Xiao, *Chin. J. Polym. Sci.* 28 (2010) 299–304.
- [15] W.-H. Sun, D. Zhang, S. Zhang, S. Jie, J. Hou, *Kinet. Catal.* 47 (2006) 278–283.
- [16] W.-H. Sun, S. Zhang, W. Zuo, *C.R. Chim.* 11 (2008) 307–316.
- [17] M. Qian, M. Wang, R. He, *J. Mol. Catal. A: Chem.* 160 (2000) 243–247.
- [18] L. LePichon, D.W. Stephan, X. Gao, Q. Wang, *Organometallics* 21 (2002) 1362–1366.
- [19] G.J.P. Britovsek, V.C. Gibson, O.D. Hoarau, S.K. Spitzmesser, A.J.P. White, D.J. Williams, *Inorg. Chem.* 42 (2003) 3454–3465.
- [20] R. Cowdell, C.J. Davies, S.J. Hilton, J.-D. Maréchal, G.A. Solan, O. Thomas, J. Fawcett, *Dalton Trans.* 20 (2004) 3231–3240.
- [21] M.-S. Zhou, S.-P. Huang, L.-H. Weng, W.-H. Sun, D.-S. Liu, *J. Organomet. Chem.* 665 (2003) 237–245.
- [22] W.-H. Sun, X. Tang, T. Gao, B. Wu, W. Zhang, H. Ma, *Organometallics* 23 (2004) 5037–5047.
- [23] L. Wang, W.-H. Sun, L. Han, H. Yang, Y. Hu, X. Jin, *J. Organomet. Chem.* 658 (2002) 62–70.
- [24] W.-H. Sun, S. Jie, S. Zhang, W. Zhang, Y. Song, H. Ma, J. Chen, K. Wedeking, R. Fröhlich, *Organometallics* 25 (2006) 666–677.
- [25] W.-H. Sun, S. Zhang, S. Jie, W. Zhang, Y. Li, H. Ma, J. Chen, K. Wedeking, R. Fröhlich, *J. Organomet. Chem.* 691 (2006) 4196–4203.
- [26] S. Jie, S. Zhang, K. Wedeking, W. Zhang, H. Ma, X. Lu, Y. Deng, W.-H. Sun, *C. R. Chim.* 9 (2006) 1500–1509.
- [27] S. Jie, S. Zhang, W.-H. Sun, X. Kuang, T. Liu, J. Guo, *J. Mol. Catal. A: Chem.* 269 (2007) 85–96.
- [28] S. Zhang, S. Jie, Q. Shi, W.-H. Sun, *J. Mol. Catal. A: Chem.* 276 (2007) 174–183.
- [29] J.D.A. Pelletier, Y.D.M. Champouret, J. Cadarso, L. Clowes, M. Ganet, K. Singh, V. Thanarajasingham, G.A. Solan, *J. Organomet. Chem.* 691 (2006) 4114–4123.
- [30] S. Jie, S. Zhang, W.-H. Sun, *Eur. J. Inorg. Chem.* (2007) 5584–5598.
- [31] W.-H. Sun, P. Hao, S. Zhang, Q. Shi, W. Zuo, X. Tang, X. Lu, *Organometallics* 26 (2007) 2720–2734.
- [32] P. Hao, S. Zhang, W.-H. Sun, Q. Shi, S. Adewuyi, X. Lu, P. Li, *Organometallics* 26 (2007) 2439–2446.
- [33] W.-H. Sun, P. Hao, G. Li, S. Zhang, W. Wang, J. Yi, M. Asma, N. Tang, *J. Organomet. Chem.* 692 (2007) 4506–4518.
- [34] S. Adewuyi, G. Li, S. Zhang, W. Wang, P. Hao, W.-H. Sun, N. Tang, J. Yi, *J. Organomet. Chem.* 692 (2007) 3532–3541.
- [35] M. Zhang, S. Zhang, P. Hao, S. Jie, W.-H. Sun, P. Li, X. Lu, *Eur. J. Inorg. Chem.* (2007) 3816–3826.
- [36] M. Zhang, P. Hao, W. Zuo, S. Jie, W.-H. Sun, *J. Organomet. Chem.* 693 (2008) 483–491.
- [37] S. Zhang, I. Vystorop, Z. Tang, W.-H. Sun, *Organometallics* 26 (2007) 2456–2460.
- [38] S. Zhang, W.-H. Sun, X. Kuang, I. Vystorop, J. Yi, *J. Organomet. Chem.* 692 (2007) 5307–5316.
- [39] K. Wang, K. Wedeking, W. Zuo, D. Zhang, W.-H. Sun, *J. Organomet. Chem.* 693 (2008) 1073–1080.
- [40] R. Gao, Y. Li, F. Wang, W.-H. Sun, M. Bochmann, *Eur. J. Inorg. Chem.* (2009) 4149–4156.
- [41] M. Zhang, R. Gao, X. Hao, W.-H. Sun, *J. Organomet. Chem.* 693 (2008) 3867–3877.
- [42] T. Xiao, J. Lai, S. Zhang, X. Hao, W.-H. Sun, *Catal. Sci. Technol.* DOI:10.1039/c1cy00028d.
- [43] S. Zhang, W.-H. Sun, T. Xiao, X. Hao, *Organometallics* 29 (2010) 1168–1173.
- [44] J. Yu, L. Hao, W. Zhang, X. Hao, W.-H. Sun, *Chem. Commun.* 47 (2011) 3257–3259.
- [45] S. Song, T. Xiao, T. Liang, F. Wang, C. Redshaw, W.-H. Sun, *Catal. Sci. Technol.* 1 (2011) 69–75.
- [46] E.Y. Chen, T.J. Marks, *Chem. Rev.* 100 (2000) 1391–1434.
- [47] A.R. Karam, E.L. Catarí, F. López-Linares, G. Agrifoglio, C.L. Albano, A. Díaz-Barrios, T.E. Lehmann, S.V. Pekarar, L.A. Albornoz, R. Atencio, T. González, H.B. Ortega, P. Joskowics, *Appl. Catal. A: Gen.* 280 (2005) 165–173.
- [48] G.J.P. Britovsek, S. Mastroianni, G.A. Solan, S.P.D. Baugh, C. Redshaw, V.C. Gibson, A.J.P. White, D.J. Williams, M.R.J. Elsegood, *Chem. Eur. J.* 6 (2000) 2221–2231.
- [49] L. Xiao, R. Gao, M. Zhang, Y. Li, X. Cao, W.-H. Sun, *Organometallics* 28 (2009) 2225–2233.
- [50] Y. Chen, P. Hao, W. Zuo, K. Gao, W.-H. Sun, *J. Organomet. Chem.* 693 (2008) 1829–1840.
- [51] G.M. Sheldrick, SHELXTL-97, Program for the Refinement of Crystal Structures. University of Göttingen, Germany, 1997.